Free-carrier and intersubband infrared absorption in p-type $Si_{1-x}Ge_x/Si$ multiple quantum wells

S. Zanier, J. M. Berroir, Y. Guldner, and J. P. Vieren
Laboratoire de Physique de la Matière Condensée, Ecole Normale Supérieure, 24 rue Lhomond, 75005 Paris, France

I. Sagnes, F. Glowacki, Y. Campidelli, and P. A. Badoz
France Telecom, Centre National d'Etudes des Télécommunications de Grenoble-CNS, Boîte Postale 98, 38243 Meylan Cedex, France
(Received 9 December 1994)

Infrared absorption has been investigated in high-quality p-type $Si_{1-x}Ge_x/Si$ multiple quantum wells grown by UHV–chemical vapor deposition. Sample parameters have been chosen in order to obtain an intersubband absorption peak at $\lambda \approx 10$ μm. Direct transmission as well as transmission through multipass waveguides have been measured for various radiation polarizations, doping levels, and temperatures. Transmission of single uniformly doped SiGe epilayers has also been performed. Both intersubband and free-carrier absorptions have been quantitatively analyzed using a modified Drude model, while the valence states have been obtained from an envelope-function formalism. The relative contributions of both free carriers and intersubband transitions to the total absorbance have been accurately determined as a function of polarization and doping level. The absorption coefficients have been deduced for radiation electric field along the growth axis and parallel to the plane of the layers. Finally, the infrared absorption at normal incidence is discussed as well as the selection rules of the intersubband transitions.

Infrared absorption in doped quantum wells has attracted a great deal of interest in the past few years because of its potential application in infrared detection in the 5–15-μm wavelength range. In addition to the $GaAs/Al_xGa_{1-x}As$ system, which has been extensively studied, much attention is now being given to the Si/SiGe system. Since in a Si/SiGe quantum-well structure grown directly onto a silicon substrate a significant band offset only occurs between the valence bands, the valence intersubband absorption has been investigated in doped SiGe quantum wells,[1–5] or in modulation-doped Si/SiGe heterostructures.[6] It has been shown in particular that valence intersubband transitions can be observed when the sample is illuminated normally to the interface planes, which is an advantage compared with the conduction intersubband transitions not allowed in normal incidence. These particular selection rules arise from the band mixing and the strain effects.[3,4,7] High p-type doping densities ($\approx 10^{19}$ cm^{-3}) are generally used in quantum-well structures designed for intersubband absorption, leading to significant free-carrier absorption. These high doping levels are necessary in order to observe transitions away from the Brillouin-zone center, where mixing of the states is noticeable. In this paper, we report a study of the infrared absorption in the range 1.5–20 μm in high-quality p-type Si/SiGe multiple quantum wells grown by UHV–chemical vapor deposition (CVD). Both intersubband and free-carrier absorptions are quantitatively analyzed. Direct transmission as well as transmission through 45° multipass waveguides are measured for various radiation polarizations, doping densities, and temperatures. The absorption spectra consist of a peak associated with the intersubband transitions superimposed on a monotonically increasing background resulting from free-carrier effects. This peak is more or less developed, depending on the radiation polarization, temperature, and doping level. In previous absorption studies,[1–6] the "free-carrier" background has not been analyzed theoretically but simply subtracted in order to magnify the intersubband absorption. Nevertheless, both effects are usually mixed over a wide spectral range, leading to an intricate situation. In order to determine the free-carrier contribution to the total infrared absorption, we have measured thick uniformly doped SiGe epilayers in addition to multiple-quantum-well structures. We have checked that a Drude model accounts perfectly for the experimental spectra both in TM and TE polarizations. We are, thus, able to accurately determine the energy position and magnitude of the intersubband transitions in the multiple-quantum-well structure as a function of polarization and sample parameters. Our experimental results are compared with the predictions of theoretical calculations.

The samples used in this study were grown, using the UHV-CVD technique, on a (100) Si substrate in a RIBER Epineat-SiGe machine. Details of this growth technique have been described elsewhere.[8,9] Both $Si_{1-x}Ge_x/Si$ multiple-quantum-well structures and single uniformly doped SiGe layers have been investigated. We present here results obtained on three samples whose parameters are listed in Table I. The parameters of samples 2 and 3

TABLE I. Sample parameters. p if the boron doping level and x is the Ge content of the SiGe layers.

Sample	Nb periods	d_{SiGe} (Å)	d_{Si} (Å)	p (cm^{-3})	x
1	SiGe	uniform	2200 Å	2×10^{19}	0.13
2	50	30	200	2×10^{19}	0.2
3	50	30	200	2×10^{18}	0.2

(50 periods, $x \approx 0.2$, well thickness ≈ 30 Å) were chosen in order to obtain a significant intersubband absorption around $\lambda = 10$ μm. The thickness and Ge content were determined by x-ray diffraction and TEM measurements.

In order to predict the energy range at which the intersubband transitions may occur, we calculated the valence energy levels at the Brillouin-zone center ($k_{\parallel} = 0$) by using a multiband envelope-function model including both Γ_8 and Γ_7 states.[10] The strain effects resulting from the 0.8% lattice parameter mismatch between $Si_{0.8}Ge_{0.2}$ and Si have been taken into account as described in Ref. 11 but we have not included the exchange interaction contribution resulting from the high doping level.[12] The values of the Luttinger parameters and the spin-orbit energy in Si and SiGe have been taken from Ref. 13. The heavy-hole valence-band offset has been assumed to be $\Delta E_v = 0.85x$ (eV).[14] Figure 1 shows a schematic diagram of the valence states calculated from the parameters (Ge content, layer thickness) of samples 2 and 3. The Γ_8 and Γ_7 band edges in Si and strained $Si_{0.8}Ge_{0.2}$ are also represented. At $k_{\parallel} = 0$, the heavy-hole states, labeled HH_n, are decoupled. The other valence states, labeled LH_n, correspond to a mixing between the light Γ_8 and Γ_7 states. The many-body effects can slightly modify the calculated energies, particularly in sample 2, which has the highest doping level. Finally, at low temperature most of the holes occupy the heavy-hole ground-state HH_1 in both samples 2 and 3.

Infrared-absorption measurements were performed at temperatures from 5 to 300 K in the spectral range 400–7000 cm^{-1} using a Fourier transform spectrometer. We first describe the direct transmission spectra, which were measured in TM polarization for a radiation incidence angle θ varying from 0° to 70° ($\approx$Brewster incidence for an air-silicon interface). For each incidence, the transmission was normalized to that of a reference boron Si substrate. Figure 2(a) shows the room-temperature transmission of sample 2 in TM polarization

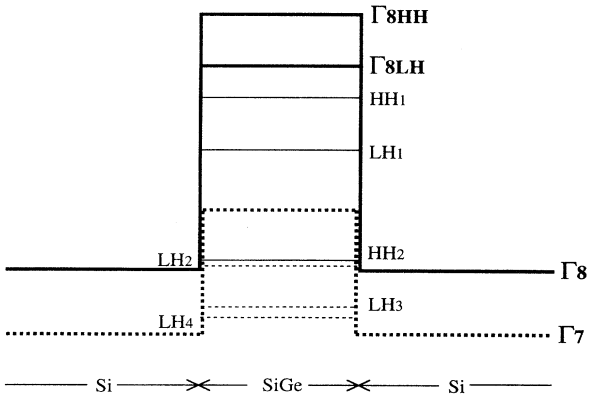

FIG. 1. Schematic representation of a $Si_{0.8}Ge_{0.2}$/Si quantum well of thickness 30 Å. The Γ_8 and Γ_7 band edges in Si and strained SiGe are represented (solid- and broken-bold lines, respectively) as well as the calculated valence states at $k_{\parallel} = 0$ (zone center).

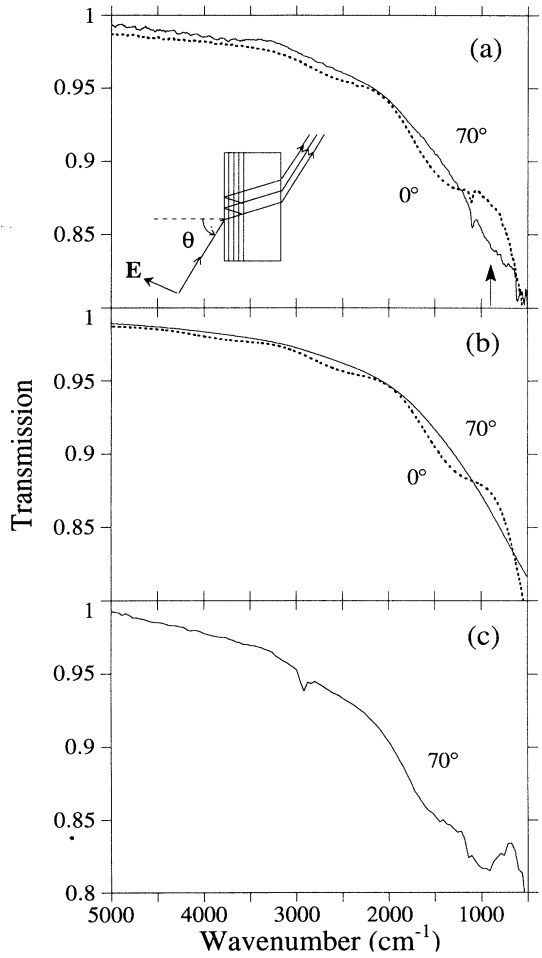

FIG. 2. (a) Direct transmission spectra of sample 2 at 300 K in TM polarization. The incidence angle (see the inset) is $\theta = 0$ (normal incidence) or $\theta = 70°$ (Brewster incidence). The arrow shows the calculated energy of the HH_1-HH_2 transition at the zone center. (b) Theoretical transmission spectra calculated from a Drude analysis. (c) Experimental TM transmission spectrum at $\theta = 70°$ and $T = 10$ K. The magnitude of the intersubband absorption at 1000 cm^{-1} is $\approx 3\%$.

at normal and Brewster incidences. The almost monotonically decreasing transmission observed for both incidences results from free-carrier effects. The oscillations visible at $\theta = 0$, which vanish at $\theta = 70°$, are associated with interferences occurring in the multiple-quantum-well structure.[9] In order to explain these data, a numerical calculation of the sample transmission including free-carrier effects, using a Drude formalism, was developed. Taking $n = 3.5$ for the Si refractive index, $\varepsilon = 12.5$ for the SiGe dielectric constant, $m^* = 0.25m_0$ for the hole effective mass in the quantum well, and the parameters of the structure given in Table I, the only adjustable parameter of the model is the carrier relaxation time τ in the doped SiGe layers. $\tau = 5 \times 10^{-15}$ s is taken for a doping level of 2×10^{19} cm^{-3}, in reasonable agreement with the mobility measurements performed at 300 K in SiGe epi-

layers with a similar doping density. The solid and broken lines in Fig. 2(b) show the results of these calculations for sample 2. The quantitative agreement with the experimental spectra [Fig. 2(a)] is almost perfect. The model accounts for the 20% drop in transmission, which results from the increasing reflection of the structure when the plasma frequency (≈ 750 cm^{-1}) is approached together with the free-carrier absorption in the doped SiGe layers. The oscillations calculated at $\theta=0$ are associated with interferences between the reflected waves in the multiple-quantum-well structure, which behaves like an effective medium with a refractive index differing more and more from the substrate index as the free-carrier absorption increases. This explains why the oscillations are enhanced near the plasma frequency. The calculation shows that no oscillation occurs at $\theta=70°$ in TM polarization, as expected at the Brewster incidence. On careful examination of Fig. 2(a), a weak broad feature can be observed in the spectra at $\theta=70°$ around 1000 cm^{-1}. This feature cannot be explained by the free-carrier effects, since it is shown in Fig. 2(b) that no feature is predicted at this energy, and must therefore be associated with the intersubband transitions. In addition, the arrow in Fig. 2(a) indicates the calculated energy of the HH_1-HH_2 transition (see Fig. 1) at the zone center, which is in good agreement with the observed weak absorption. This assumption is fully confirmed by the low-temperature measurements, as can be seen on the transmission spectrum at $T=10$ K and $\theta=70°$ shown in Fig. 2(c). The magnitude of the absorption line around 1000 cm^{-1} is clearly enhanced ($\approx 3\%$), whereas the linewidth decreases because of the reduced thermal broadening. At $\theta=0$, the interference effects prevent any accurate determination of the intersubband absorption, essentially because a transmission maximum occurs around 900 cm^{-1} [see Figs. 2(a) and 2(b)]. Nevertheless, a small absorption can be observed at $T=10$ K within the interference maximum, demonstrating the existence of intersubband transitions at normal incidence. However, direct transmission measurements are clearly not sufficient to determine the magnitude and selection rules of the intersubband transitions as a function of polarization, essentially because the radiation electric field component along the growth axis is either zero ($\theta=0$) or very small (at $\theta=0°$, the internal incidence angle is only $\approx 15°$).

In order to determine the influence of the electric-field direction on absorption, we used multipass waveguides of 2.5 mm in length (2 mm for sample 1) and 0.5 mm in thickness with 45° facets. With a normal incidence on the facet (see inset of Fig. 3), the propagation angle inside the multiple-quantum-well structure is 45°. As a result, the infrared beam passes five times (four times for sample 1) through the quantum wells, thus enhancing the absorption. Measurements were performed for various electric-field angles from $\phi=0$ (TM configuration, see inset of Fig. 3) to $\phi=90°$ (TE configuration). In TE geometry, the electric field is parallel to the layer planes, while in TM configuration it has equal components along the structure growth axis and parallel to the layers. All spectra were normalized to that of a reference Si substrate

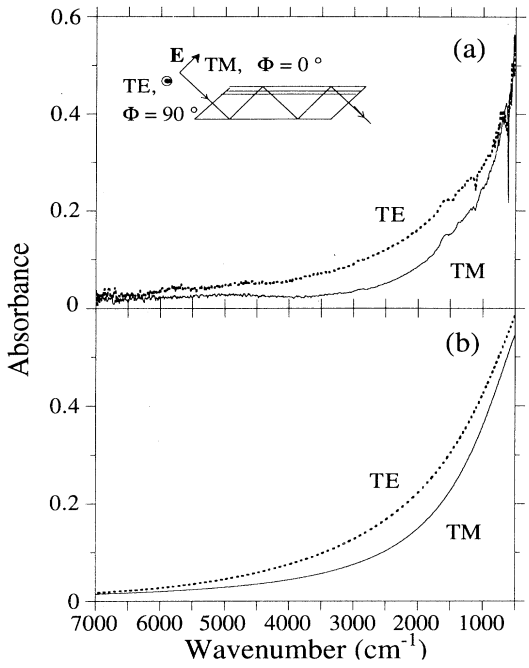

FIG. 3. (a) Absorbance at 300 K of sample 1, which is uniformly doped SiGe epilayer. The inset is a sketch of the multipass waveguide geometry where the radiation polarization angle Φ is defined. (b) Theoretical absorbance calculated for the parameters of sample 1.

waveguide of similar length and thickness in order to eliminate the substrate absorption. The free-carrier effects alone were first measured in sample 1, which consists of a single 0.22-μm-thick SiGe layer uniformly doped at 2×10^{19} cm^{-3} (see Table I). Such a layer is quite comparable (thickness and doping) to the total number of SiGe layers in multiple-quantum-well structure No. 2. Its room-temperature absorbance (i.e., logarithm of the normalized transmission) is shown in Fig. 3(a) in both TE and TM configurations. At a given photon energy, the free-carrier absorption is $\approx 4\sqrt{2}$ times higher than in direct transmission, in quantitative agreement with the total length of doped SiGe through which the infrared beam passes due to multiple reflections. Figure 3(b) presents the calculated absorption of the waveguide using the Drude model described above and a carrier relaxation time of $\tau=5\times10^{-15}$ s. Again, the agreement with the experiments is good. The different absorbances in TE and TM geometries arise from the dependence of the doped layer reflection coefficient on the polarization.

Once sure of accounting for the free-carrier effects in a simple SiGe epilayer, we analyzed the transmission of the multiple-quantum-well structures in waveguide geometry. Figure 4(a) shows the absorbance of sample 2 measured at 300 K for various polarization angles ϕ. In addition to the free-carrier effects, giving a monotonically increasing absorbance with decreasing wave number, a well-developed peak can be observed around 1000 cm^{-1} in TM configuration ($\Phi=0$) corresponding to the intersub-

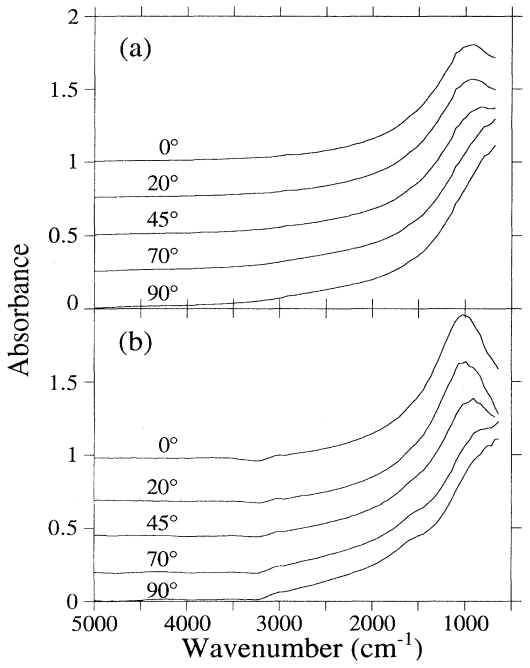

FIG. 4. (a) Room-temperature absorbance of sample 2 measured in waveguide geometry for various polarization angles Φ. For the sake of clarity, the curves are shifted vertically one with respect to the other. (b) Similar spectra at $T=10$ K. The peak around 1000 cm^{-1} corresponding to intersubband transitions is enhanced.

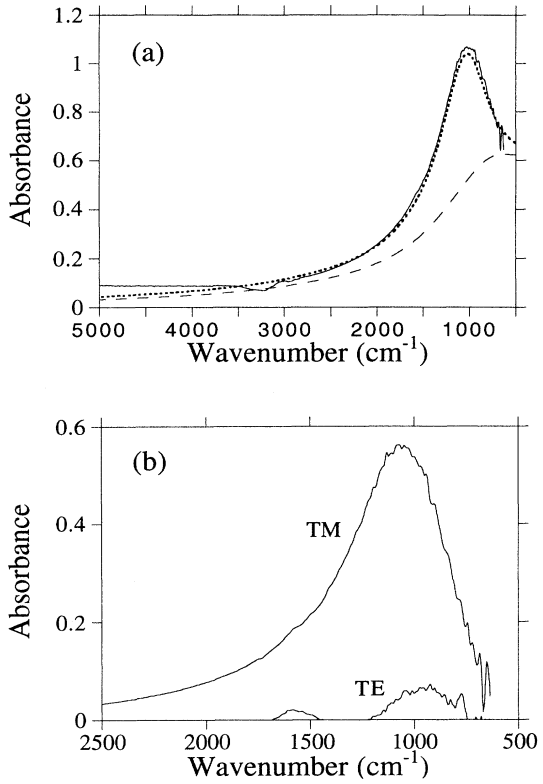

FIG. 5. (a) Comparison of the TM absorbance of sample 2 (waveguide) at 10 K (solid line) with the calculated absorbance (dotted line) using a modified Drude model. The broken line represents the calculated free-carrier contribution to the total absorbance. (b) Intersubband contribution to the total infrared absorbance determined at $\Phi=0°$ (TM) and $\Phi=90°$ (TE) in sample 2 at $T=10$ K.

band transitions. This peak becomes weaker as Φ increases and almost vanishes at $\Phi=90°$ (TE), showing that the intersubband transitions are stronger for a radiation electric field along the growth axis than for an electric field parallel to the layers. The TM intersubband absorption is considerably magnified compared to the direct transmission measurements shown in Fig. 1(a). This enhancement is quantitatively explained by the increasing total number of quantum wells through which the infrared beam passes due to the multiple reflections, and by the 45° incidence angle, which significantly enhances the electric-field component along the growth axis. In order to reduce the thermal broadening of the peak and to measure the intersubband absorption at $\Phi=90°$, we carried out similar experiments at lower temperature, as seen in Fig. 4(b), which presents the absorbance at $T=10$ K. The peak is sharper than at room temperature and a weak intersubband absorbance can now be observed at $\Phi=90°$. In order to quantitatively analyze these data, we modified the Drude transmission model described above. The intersubband absorption is then included by adding a Lorentzian contribution κ to the imaginary part of the refractive index of the doped SiGe layers. The position, amplitude, and width of this Lorentzian function are used as adjustable parameters and the intersubband absorption coefficient is determined from the fitting procedure. Figure 5(a) presents a comparison of the experimental TM data at 10 K (solid line) with the calculated absorbance (dotted line) using a carrier relaxation time $\tau=5\times10^{-15}$ s and a Lorentzian contribution centered at 1000 cm^{-1} with a peak value $\kappa_{max}=0.75$ and a half-width at half amplitude (HWHA) of 250 cm^{-1}. The agreement is almost excellent. The small discrepancy observed at high wave number could be explained by some light diffusion effects resulting from the nonperfect polishing of the sample facets. The broken line represents the free-carrier absorbance alone, corresponding to $\kappa=0$ in our calculations. It is important to point out that this free-carrier contribution does not correspond to a simple "numerical background" and that our Drude analysis is crucial for the accurate measurement of the intersubband absorption. Note also that around 1000 cm^{-1} ($\lambda=10$ μm), the free carriers and intersubband transitions contribute equally to the TM absorbance in sample 2. This observation is of particular interest for interpretation of the results obtained in the quantum-well infrared photodetectors.[15] A similar analysis can be made for each polarization angle Φ. The intersubband contribution alone [obtained, for instance, at $\Phi=0$ from the difference between the solid and broken lines in Fig. 5(a)] is shown in Fig. 5(b) at both $\Phi=0$ and $\Phi=90°$. The TM peak is rather broad (HWHA$\approx$250 cm^{-1}), resulting from the nonparabolicity

of the valence subbands and the high doping level, which allows transitions well away from the Brillouin-zone center. Such a width is characteristic of the valence transitions and is considerably larger than that measured for the conduction intersubband absorption.[16,17] Recent calculations by Corbin, Wong, and Jaros[18] in p-type $Si_{1-x}Ge_x/Si$ quantum wells have predicted a similar large absorption width for a doping level of around 10^{19} cm^{-3}, even without taking into account the imperfections at the interfaces and other possible defects. A rather small change in intersubband absorption with temperature was measured as shown in Figs. 4(a) and 4(b). Only a thermal broadening of the peak can be observed, which is also in fairly good agreement with the calculations of Corbin, Wong, and Jaros. The maximum intersubband absorbance at 1000 cm^{-1} shown in Fig. 5(b) is ≈ 0.6 in TM and ≈ 0.06 in TE, corresponding to absorption coefficients in the doped SiGe layers of $\alpha_{TM} \approx 9400$ cm^{-1} and $\alpha_{TE} \approx 900$ cm^{-1}, respectively. If one considers the 45° incidence angle in the guide, the absorption coefficient for polarization along the growth axis is found to be $\alpha_z \approx 18\,000$ cm^{-1}. This coefficient is much higher than $\alpha_{\parallel} = \alpha_{TE}$ for a polarization parallel to the layers. These values are quite consistent with the direct transmission measurements shown in Fig. 2(c). For instance at $\theta = 70°$, the internal propagation angle is $\approx 15°$ leading to $\approx 4\%$ intersubband absorption at 1000 cm^{-1} in fairly good agreement with the measurements. Moreover, the ratio $\alpha_z/\alpha_{\parallel} \approx 20$ demonstrates that intersubband transitions do occur at normal incidence but that the corresponding absorption coefficient is rather low, at least for $Si_{0.8}Ge_{0.2}/Si$ multiple-quantum-well structures designed for a peak absorption at $\lambda = 10$ μm. Indeed, at $\Phi = 90°$, it is clear from Figs. 4(b) and 5(b) that most of the infrared absorption around 1000 cm^{-1} arises from free carriers. This is particularly important for the potential applications to normal incidence infrared detection. It has been shown recently[19] that high normal-incidence intersubband absorption can be obtained by increasing the Ge content in the SiGe alloy of the quantum well but the peak response is then centered at a shorter wavelength (≈ 3 μm).

Finally we have also investigated the influence of the quantum-well doping. For instance, sample 3 is similar to sample 2 with a doping level one order of magnitude smaller (see Table I). We first analyzed the free-carrier absorption obtained in the waveguide geometry for TM and TE polarizations using our Drude model and checked that the spectra can be interpreted with $\tau = 10^{-14}$ s as carrier relaxation time. We then determined, as described above, the intersubband contribution, which is shown in Fig. 6 at 10 K for both TM and TE geometries. The magnitude of the TM peak is lower than in sample 2 (0.12 instead of 0.6 absorbance) and the peak presents well-defined structures, which correspond to various transitions. The two arrows in Fig. 6 show the calculated energy at the zone center of transitions HH_1-HH_2 or HH_1-LH_2 (≈ 910 cm^{-1}) and HH_1-LH_3 or HH_1-LH_4 (≈ 1130 cm^{-1}), where the subbands are labeled as described in Fig. 1. Note that the HH_1-HH_2 transition, which is the dominant one at TM polarization,[18] occurs

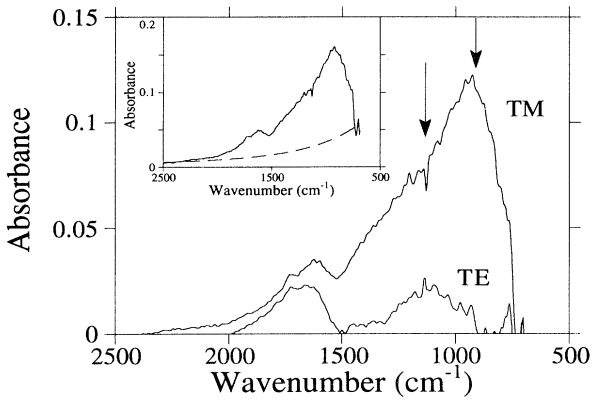

FIG. 6. Intersubband contribution to the total absorbance measured at $T = 10$ K in sample 3 (waveguide). The arrows show the calculated energies at the zone center of the ground intersubband transitions. The inset presents the total TM absorbance (solid line) and, for comparison, the calculated free-carrier background (broken line).

at ≈ 900 cm^{-1} in sample 3 and ≈ 1000 cm^{-1} in sample 2. This shift towards high energy is most probably due to the exchange interaction effects, which are strongly dependent on the free-carrier density.[12] The peak observed at higher energy (≈ 1600 cm^{-1}) arises probably from a transition between HH_1 and the continuum states. The inset in Fig. 6 shows the total TM absorbance (solid line) and the calculated free-carrier background (broken line). Contrary to sample 2, the intersubband absorbance becomes the dominant contribution at ≈ 900 cm^{-1}, essentially because of the weak free-carrier contribution (≈ 0.05 absorbance). A small intersubband absorbance (≈ 0.02) was measured in TE polarization, where two structures can be observed (Fig. 6) corresponding to HH_1-LH_3 (or HH_1-LH_4) and to a transition between HH_1 and the continuum states, respectively. The HH_1-HH_2 transition, dominant in TM, almost vanishes in TE. In order to provide a more accurate description of these structures, detailed calculations of the transition strengths away from the zone center would be necessary. As for sample 2, the free carriers mainly contribute to the total TE infrared absorption.

In summary, we have presented an analysis of the infrared absorption in p-type $Si_{1-x}Ge_x/Si$ multiple quantum wells defined for a peak absorption at $\lambda \approx 10$ μm. Direct transmission as well as transmission through multipass waveguides have been measured. Using a Drude model, we have accurately determined the free-carrier contribution, from which the intersubband absorption can be obtained as a function of the radiation polarization. For a high doping level (a few 10^{19} cm^{-3}), we have demonstrated that the free carriers and intersubband transitions contribute equally to the TM absorbance around $\lambda = 10$ μm, whereas the TE absorbance is essentially governed by the free-carrier effects. Intersubband transitions can be observed in normal incidence but the corresponding absorption coefficient is found to be rather

small. For a lower doping density (a few 10^{18} cm^{-3}), the intersubband absorption becomes the dominant contribution in TM polarization, even if the corresponding absorption coefficient is smaller. The free-carrier effects remain the main contribution to the TE absorption. The intersubband absorption presents structures that can be associated with different transitions. These results are important for the potential applications of $Si_{1-x}Ge_x/Si$ multiple-quantum-well structures to infrared detection. Indeed both intersubband excitation and internal photoemission of holes excited via free-carrier absorption play a key role in the photoresponse of the quantum-well infrared detectors.

This work has been funded in part by the Direction des Recherches, Etudes et Techniques (DRET). The Laboratoire de Physique de la Matière Condensée at the Ecole Normale Supérieure is associated with the CNRS and the University Paris 6.

[1]R. P. G. Karunasiri, J. S. Park, Y. J. Mii, and K. L. Wang, Appl. Phys. Lett. **57**, 2585 (1990).
[2]J. S. Park, R. P. G. Karunasiri, and K. L. Wang, Appl. Phys. Lett. **60**, 103 (1992).
[3]J. S. Park, R. P. G. Karunasiri, and K. L. Wang, Appl. Phys. Lett. **61**, 681 (1992).
[4]R. People, J. C. Bean, C. G. Bethea, S. K. Sputz, and L. J. Peticolas, Appl. Phys. Lett. **61**, 1122 (1992).
[5]S. K. Chun, D. S. Pan, and K. L. Wang, Appl. Phys. Lett. **62**, 1119 (1993).
[6]T. Fromhertz, E. Koppensteiner, M. Helm, G. Bauer, J. F. Nützel, and G. Abstreiter, Solid-State Electron. **37**, 941 (1994); also in Jpn. J. Appl. Phys. **33**, 2361 (1994).
[7]Y. C. Chang and R. B. James, Phys. Rev. B **39**, 12 672 (1989).
[8]F. Glowacki, A. Larre, F. Ferrieu, Y. Campidelli, and D. Ben Sahel, in *Rapid Thermal and Integrated Processing III,* edited by J. J. Wortman, J. C. Gelpey, M. L. Green, S. R. J. Brueck and F. Roozeboom, MRS Symposia Proceedings No. 342 (Materials Rsearch Society, Pittsburgh, 1994), p. 69.
[9]I. Sagnes, Ph.D. thesis, Université Joseph Fourier, 1994.
[10]G. Bastard, *Wave Mechanics Applied to Semiconductor Heterostructure* (Les Editions de Physique, Paris, 1988).
[11]R. People, Phys. Rev. B **32**, 1405 (1985).
[12]K. M. S. V. Bandara, D. D. Coon, O. Byungsung, Y. F. Lin, and M. H. Francombe, Appl. Phys. Lett. **53**, 1931 (1988).
[13]*Semiconductors. Physics of Group IV Elements and III-V Compounds,* edited by K.-H. Hellwege and O. Madelung, Landolt-Börnstein, New Series, Group III, Vol. 17, Pt. a (Springer-Verlag, Berlin, 1982).
[14]Y. Guldner, J. M. Berroir, J. P. Vieren, M. Voos, I. Sagnes, P. A. Badoz, P. Warren, and D. Dutartre, Phys. Rev. B **48**, 12 312 (1993).
[15]R. P. G. Karunasiri, J. S. Park, and K. L. Wang, Appl. Phys. Lett. **59**, 2588 (1991).
[16]B. F. Levine, R. J. Malik, J. Walker, K. K. Choi, C. G. Bethea, D. A. Kleinman, and J. M. Vandenberg, Appl. Phys. Lett. **50**, 273 (1987).
[17]H. Hertle, G. Schuberth, E. Gornik, G. Abstreiter, and F. Schäffler, Appl. Phys. Lett. **59**, 2977 (1991).
[18]E. Corbin, K. B. Wong, and M. Jaros, Phys. Rev. B **50**, 2339 (1994).
[19]R. P. G. Karunasiri, J. S. Park, and K. L. Wang, Appl. Phys. Lett. **61**, 2434 (1992).